Food Chemistry 138 (2013) 2260–2266

Contents lists available at SciVerse ScienceDirect

Food Chemistry

journal homepage: www.elsevier.com/locate/foodchem

Biotransformation of imperatorin by *Penicillium janthinellum*. Anti-osteoporosis activities of its metabolites

Xia Lv [a,1], Dan Liu [b,1], Jie Hou [a], Peipei Dong [c], Libin Zhan [c], Li Wang [a], Sa Deng [a], Changyuan Wang [a], Jihou Yao [a], Xiaohong Shu [a], Kexin Liu [a], Xiaochi Ma [a,c,*]

[a] College of Pharmacy, Dalian Medical University, Dalian 116044, China
[b] School of Science, Dalian Nationalities University, Dalian 116600, China
[c] Research Institute of Integrated Traditional and Western Medicine, Dalian Medical University, Dalian 116044, China

ARTICLE INFO

Article history:
Received 13 October 2012
Received in revised form 26 November 2012
Accepted 28 November 2012
Available online 28 December 2012

Keywords:
Penicillium janthinellum
Biotransformation
Coumarin
Imperatorin
Anti-osteoporosis activity

ABSTRACT

Imperatorin (**IMP**) is a major constituent of many herbal medicines and possesses anti-osteoporosis activity. The present research work aimed to study the biotransformation processes of **IMP** and evaluated the anti-osteoporosis activity of the transformed metabolites. Among 18 strains of filamentous fungi screened, *Penicillium janthinellum* AS 3.510 exhibited good capability to metabolise **IMP** to the new derivatives. Ten transformed products were isolated and purified, and their structures were identified accurately based on spectroscopic data. Eight metabolites (**2–8** and **10**) were novel and previously unreported. The major biotransformation reactions involved hydroxylation of the prenyloxy side-chain and the lactone ring-opening reaction of furocoumarin skeleton. In addition, anti-osteoporosis activities of all products (**1–10**) were evaluated using MC3T3-E1 cells. The results showed that products **5** and **8** had the best bioactivities in increasing MC3T3-E1 cell growth. These products could be used in future therapeutic regimens for treating osteoporosis.

1. Introduction

Imperatorin (**IMP**) is a linear furanocoumarin, with a chemical structure of 8-isopentenyloxypsoralen (9-(3-methylbut-2-enyloxy)-7H-furo [3,2-g] chromen-7-one). **IMP** naturally exists in many Chinese herbal medicines, especially *Angelica dahurica*, *Cnidium monnieri* (L.) Cusson and *Imperatoria osthruthium*. These have been widely used as medicines and functional foods for the treatment of osteoporosis, relief of swelling and pain (He, Zhang, He, & Cao, 2007). The potential pharmacological activities of **IMP** included anti-osteoporosis activity (Tang, Yang, Chen, Chen, & Fu, 2008; Zhang & Qin, 2003), antitumour (Kim, Kim, & Ryu, 2007), anti-inflammatory (Garcia-Argaez, Ramirez-Apan, Delgado, Velazquez, & Martinez-Vazquez, 2000) and antimicrobial effects (Rosselli et al., 2006), β-secretase (BACE1) inhibitory activity (Marumoto & Miyazawa, 2010a), inhibition of myocardial hypertrophy (Zhang, Cao, Zhan, Duan, & He, 2010), and effects on drug-metabolising enzymes (Shin & Woo, 1986). However, its poor solubility and oral availability in water limit its use clinically or as a foodstuff (Li, 2006).

Biotransformation has become an economically competitive technology for modifying chemical compounds with complex structures. It possesses the advantages of high regio- and stereoselectivity, mild reaction conditions, and simple operation procedures. In recent years, our research group has frequently reported structural modifications of natural functional products to obtain new chemical entities with better bioactivity and improved water solubility (Deng et al., 2012; Li et al., 2011; Ma, Cui, Zheng, & Guo, 2007; Ma, Wu, & Guo, 2006; Ma, Xin, Liu, Han, & Guo, 2008; Ma, Zheng, & Guo, 2007; Ma et al., 2011).

In the present research, *Penicillium janthinellum* AS 3.510 exhibited good capabilities to transform **IMP**. Ten transformed products of **IMP** were isolated and identified, including eight novel metabolites **2–8** and **10** (Fig. 1). Regio-specific hydroxylation, hydrolysis, methylation, hydrogenation and glycosylation reactions of **IMP** by suspended-cell cultures of *P. janthinellum* AS 3.510 were reported. The anti-osteoporosis activities of all transformed products were evaluated by using MC3T3-E1 cells, and preliminary structure–activity relationships were concluded. Some new metabolites (**5** and **8**) of **IMP** with potent bioactivity could be used as preferred candidates for development of new functional foods or drugs.

2. Materials and methods

2.1. Apparatus

1D and 2D NMR spectra were determined in dimethylsulfoxide-d_6 (DMSO-d_6) by a Bruker ARX 600 NMR spectrometer with

* Corresponding author at: College of Pharmacy, Dalian Medical University, Lvshun South Road No. 9, Dalian 116044, China. Tel./fax: +86 411 86110419.
E-mail address: maxc1978@163.com (X. Ma).
[1] These authors contributed equally to this work.

0308-8146/$ - see front matter © 2012 Elsevier Ltd. All rights reserved.
http://dx.doi.org/10.1016/j.foodchem.2012.11.138

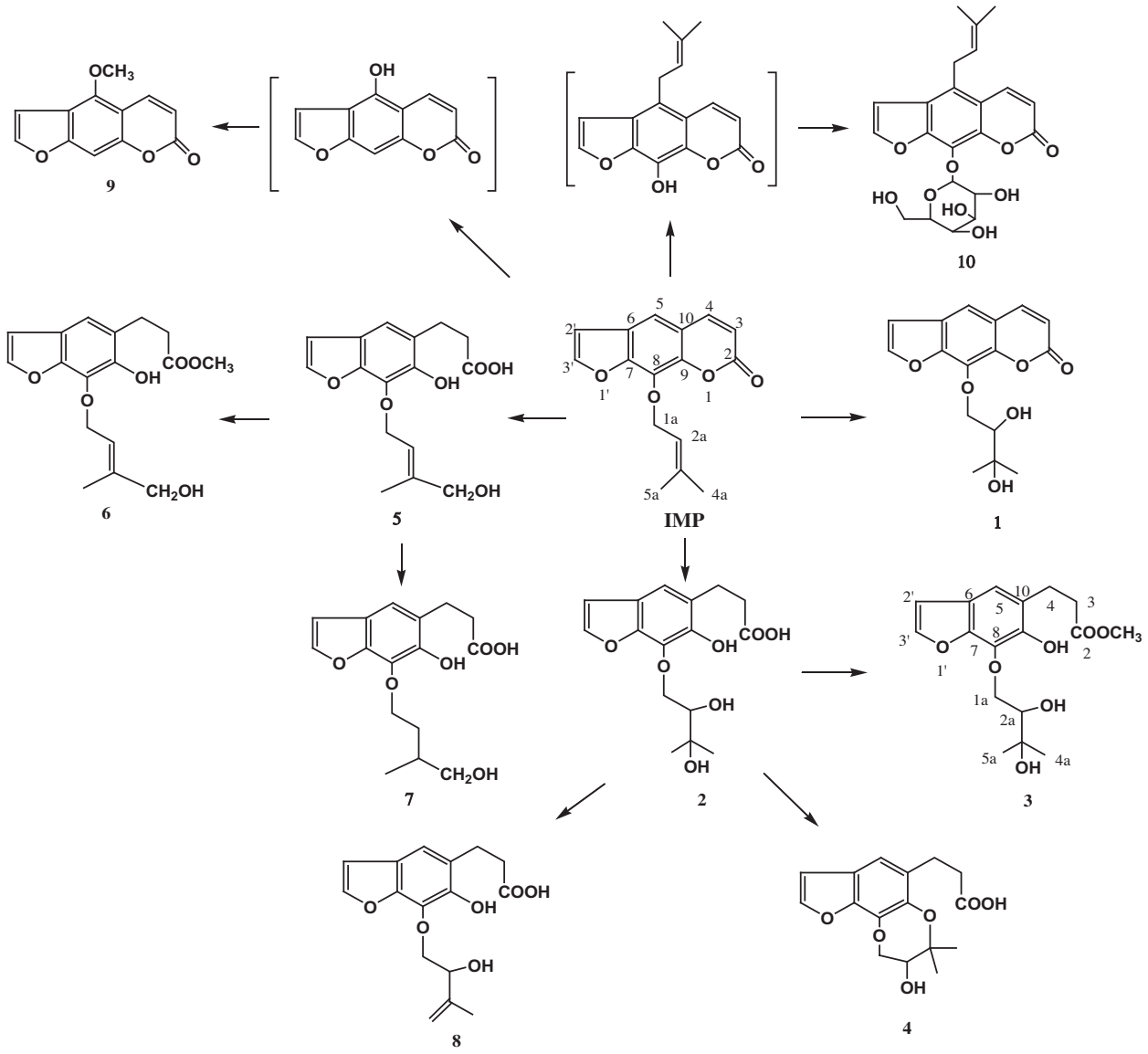

Fig. 1. Biotransformation products of **IMP** by *P. janthinellum* AS 3.510.

tetramethylsilane (TMS) as internal standard. Electrospray ionisation mass spectrometry (ESI-MS) was performed using an API3200 mass spectrometer (AB SCIEX, Framingham, MA). HRMS data were obtained using a Bruker APEXII Fourier transform ion cyclotron resonance (FT-ICR) mass spectrometer. HPLC analyses were performed on an UltiMate 3000 instrument (Thermo Scientific Dionex) equipped with a diode array detector. Melting points were measured on an XT4A apparatus (Dianguang Corp., Shanghai, China) and were uncorrected. Optical rotations were measured using a Perkin-Elmer 243B polarimeter. Ultraviolet (UV) spectra were detected on a TU-1091 UV–visible spectrophotometer. Infrared (IR) spectra were obtained on an Avatar 360 FT-IR spectrophotometer (Thermo Nicolet).

2.2. Reagents

All organic solvents were of analytic grade and were obtained from Tianjing Chemical Company (China). For HPLC experiments, chromatographic grade acetonitrile and methanol (Merck, Darmstadt, Germany) were used. Thin-layer chromatography (TLC) analyses were performed on silica gel GF254 (300–400 mesh), which was purchased from Qingdao Marine Chemical Corporation, China. Octadecylsilane (ODS) was purchased from YMC Co., Ltd. (Kyoto, Japan). **IMP** was isolated from *C. monnieri* (L.) Cusson using HPLC analysis by the author (X. Lv), with >98% purity. Icariside with 98% purity was purchased from the National Institutes for Food and Drug Control, Beijing, China.

2.3. Microorganisms

Alternaria alternata AS 3.577, *Alternaria alternata* AS 3.4578, *Aspergillus niger* AS 3.795, *Aspergillus candidus* CICC 2360, *Cunninghamella blakesleeana* Lendner AS 3.970, *Cunninghamella elegans* AS 3.1207, *Cunninghamella elegans* AS 3.2028, *Fusarium solani* AS 3.1829, *Mucor spinosus* AS 3.3450, *Mucor spinosus* AS 3.2450, *Mucor spinosus* AS 3.3447, *Mucor subtilissimus* AS 3.2454, *Mucor subtilissimus* AS 3.2456, *Mucor polymorphosporus* AS 3.3443, *Penicillium janthinellum* AS 3.510, *Penicillium aurantigriseum* AS 3.4512, *Rhizopus stolonifer* AS 3.2050 and *Trichoderma viride* AS 3.2942 were purchased from the Chinese General Microbiological Culture Collection Center, Beijing, China.

2.4. Culture medium

All culture and biotransformation experiments were performed in liquid potato medium. Minced and husked potato (200 g) was boiled in water for 1 h, and the solution was filtered. The filtrate was added to 1 L of water after adding 20 g of glucose.

2.5. Culture and biotransformation procedures

Screening scale biotransformation of **IMP** was carried out in 250-mL Erlenmeyer flasks containing 100 mL of liquid medium. The flasks were placed on a rotary shaker operating at 180 rpm and 27 °C. The substrates were dissolved in acetone to reach a final concentration of 10 mg/mL. After 36 h of pre-culture, 2 mg of **IMP** were added into each flask. The incubation was allowed to continue for 5 days. Culture controls consisted of fermentation blanks with microorganisms grown under identical non-substrate conditions. Substrate controls were composed of sterile medium with substrate, and they were incubated without microorganisms.

Preparative scale biotransformation of **IMP** by *P. janthinellum* AS 3.510 was carried out in a 1-L Erlenmeyer flask. The substrate (10 mg) dissolved in acetone (0.5 mL) was added to pre-cultured medium (400 mL) and was incubated for an additional 5 days. In total, 800 mg of substrate were used for the preparative scale biotransformation. Other procedures were similar to the screening scale biotransformation.

2.6. Extraction, purification and identification of major biotransformed products

The culture was filtered and the filtrate was extracted four times with the same volume of ethyl acetate (EtOAc). The organic phase was collected and concentrated under reduced pressure at 40 °C. The brown residues obtained (1.4 g) were applied to an octadecylsilane (ODS) column eluting with MeOH–H_2O (in a gradient manner from 10:90 to 90:10) to give 50 fractions. Based on the results of HPLC analysis, the biotransformed metabolites of **IMP** were detected in Fr 17–39. Then, Fr 17–28 were successively purified by semi-preparative HPLC (mobile phase: 45% acetonitrile in 0.03% aqueous acetic acid; flow rate: 1.5 mL/min) to afford compound **1** (25 mg, 3.1%) and six small fractions, which were further subjected to semi-preparative HPLC (mobile phase: 40% acetonitrile in 0.03% aqueous acetic acid; flow rate: 2.0 mL/min) to give compounds **2** (8.0 mg, 1.0%), **3** (4.0 mg, 0.5%), **4** (5.0 mg, 0.63%), **5** (6.0 mg, 0.75%), **6** (3.5 mg, 0.4%) and **7** (3.0 mg, 0.37%). Successful purification of Fr 29–39 by semi-preparative HPLC with 50% acetonitrile in 0.03% aqueous acetic acid as mobile phase and flow rate of 1.5 mL/min yielded compounds **8** (3.0 mg), **9** (5.0 mg, 0.63%) and **10** (4.5 mg, 0.56%). A large quantity of substrates was detected in the mycelium rather than the culture liquid. About 230 mg of substrates were obtained from the mycelium of *P. janthinellum* AS 3.510. All the products were identified based on their spectral data. The ^{1}H and ^{13}C NMR spectral data are given in Tables 1 and 2.

2.6.1. 6,7-Furano-8-(2a,3a-dihydroxyprenyloxy)hydrocoumaric acid (**2**)

Yellow powder, m.p. 215–217 °C, $[\alpha]_D^{22}$ −18.7 (*c* = 0.2, MeOH); UV λ_{max} (MeOH): 210, 252 and 286 nm. ^{1}H NMR (DMSO-d_6, 600 MHz) and ^{13}C NMR (DMSO-d_6, 150 MHz) see Tables 1 and 2. HRESIMS $[M-H]^-$ *m/z* 323.1135 (calcd. for $C_{16}H_{19}O_7$, 323.1131).

2.6.2. 6,7-Furano-8-(2a,3a-dihydroxyprenyloxy)hydrocoumaric acid methyl ester (**3**)

Yellow powder, m.p. 205–206 °C, $[\alpha]_D^{22}$ −23.5 (*c* = 0.2, MeOH); UV λ_{max} (MeOH): 210, 252 and 286 nm. ^{1}H NMR (DMSO-d_6, 600 MHz) and ^{13}C NMR (DMSO-d_6, 150 MHz) see Tables 1 and 2. HRESIMS $[M-H]^-$ *m/z* 337.1290 (calcd. for $C_{17}H_{21}O_7$, 337.1287).

2.6.3. 6,7-Furano-8-(2a-hydroxy-3a,9-epoxyprenyloxy)hydrocoumaric acid (**4**)

Yellow powder, m.p. 197–198 °C, $[\alpha]_D^{22}$ −10.4 (*c* = 0.2, MeOH); UV λ_{max} (MeOH): 212, 253 and 280 nm. ^{1}H NMR (DMSO-d_6, 500 MHz) and ^{13}C NMR (DMSO-d_6, 125 MHz) see Tables 1 and 2. HRESIMS $[M-H]^-$ *m/z* 305.1017 (calcd. for $C_{16}H_{18}O_6$, 305.1025).

2.6.4. 6,7-Furano-8-(5a-hydroxymethylprenyloxy)hydrocoumaric acid (**5**)

Yellow powder, m.p. 227–228 °C, $[\alpha]_D^{22}$ −2.5 (*c* = 0.3, MeOH); UV λ_{max} (MeOH): 205, 252 and 286 nm. ^{1}H NMR (DMSO-d_6, 600 MHz) and ^{13}C NMR (DMSO-d_6, 150 MHz) see Tables 1 and 2. HRESIMS $[M-H]^-$ *m/z* 305.1021 (calcd. for $C_{16}H_{18}O_6$, 305.1025).

2.6.5. 6,7-Furano-8-(5a-hydroxymethylprenyloxy)hydrocoumaric acid methyl ester (**6**)

Yellow powder, m.p. 198–199 °C, $[\alpha]_D^{22}$ −1.5 (*c* = 0.1, MeOH); UV λ_{max} (MeOH): 206, 252 and 286 nm. ^{1}H NMR (DMSO-d_6, 600 MHz) and ^{13}C NMR (DMSO-d_6, 150 MHz) see Tables 1 and 2. HR-ESIMS $[M-H]^-$ *m/z* 305.1021 (calcd. for $C_{16}H_{18}O_6$, 305.1025).

2.6.6. 6,7-Furano-8-(5a-hydroxymethyl-2a,3a-dihydroprenyloxy)hydrocoumaric acid (**7**)

Yellow powder, m.p. 205–206 °C, $[\alpha]_D^{22}$ −9.5 (*c* = 0.1, MeOH); UV λ_{max} (MeOH): 210, 253 and 285 nm. ^{1}H NMR (DMSO-d_6, 600 MHz) and ^{13}C NMR (DMSO-d_6, 150 MHz) see Tables 1 and 2. HRESIMS $[M-H]^-$ *m/z* 307.1185 (calcd. for $C_{16}H_{20}O_6$, 307.1182).

2.6.7. 6,7-Furano-8-(2a-hydroxy-3a-en-prenyloxy)hydrocoumaric acid (**8**)

Yellow powder, m.p. 221–222 °C, $[\alpha]_D^{22}$ −12.5 (*c* = 0.1, MeOH); UV λ_{max} (MeOH): 209, 253 and 286 nm. ^{1}H NMR (DMSO-d_6, 600 MHz) and ^{13}C NMR (DMSO-d_6, 150 MHz) see Tables 1 and 2. HRESIMS $[M-H]^-$ *m/z* 305.1028 (calcd. for $C_{16}H_{18}O_6$, 305.1025).

2.6.8. 6,7-Furano-5-isopentylcoumarin 8-O-β-D-glucoside (**10**)

Yellow powder, $[\alpha]_D^{22}$ +35.5 (*c* = 0.1, MeOH); UV λ_{max} (MeOH): 222, 252 and 311 nm. ^{1}H NMR (DMSO-d_6, 600 MHz) and ^{13}C NMR (DMSO-d_6, 150 MHz) see Tables 1 and 2. HRESIMS $[M-H]^-$ *m/z* 455.1314 (calcd. for $C_{22}H_{25}O_9$, 455.1318).

2.7. Analysis methods

The samples were analysed on an Ultimate 3000 HPLC equipped with a Dionex C-18 column (inner diameter: 4.6 mm, length: 250 mm, and particle size: 5 μm), and DAD at 285 nm. The eluting procedure was performed as follows: initial elution for 0–5 min with MeOH:H_2O (40:60, v/v), linear change from MeOH:H_2O (40:60, v/v) to (55:45, v/v) for 5–25 min, isocratic elution (55:45, v/v) for next 25–35 min, and a linear change to MeOH:H_2O (90:10, v/v). The flow rate was 0.8 mL/min and column temperature was 30 °C.

2.8. Acid hydrolysis

Acid hydrolysis of the glycosides was carried out by refluxing 1.0 mg of glycoside **10** in 5 mL of 6% hydrochloric acid in MeOH for 4 h. The reaction mixture was partitioned by EtOAc (20 ml). The aqueous layer was evaporated and developed with $CHCl_3$:-MeOH:H_2O (15:7:2, v/v/v). Sugars were detected using thymol in H_2SO_4 (0.5 g thymol in 95 mL of EtOH and 5 mL of H_2SO_4) followed by heating the plates at 120 °C for 10 min, and were identified as sugar moieties by co-chromatography with reference samples.

Table 1
^{1}H NMR spectral data for **IMP** and **1–10** (DMSO-d_6, 600 MHz, δ in ppm, J in Hz).

H	Imperatorin	1	2	3	4	5	6	7	8	9	10
3	6.32d(9.5)	6.41d(9.5)	2.51 m	2.60t(8.0,7.5)	2.51 m	2.49 m	2.58t(8.0,7.5)	2.50 m	2.52 m	6.31d (10.0)	6.43d (10.0)
4	7.71d(9.5)	8.12 d(9.5)	2.84t(7.5,8.0)	2.87t(7.5)	2.88 m	2.82t(7.5)	2.85t(8.0,7.5)	2.84 m	2.83t (7.5)	8.19d (10.0)	8.20 d (10.0)
5	7.31s	7.06s	7.03s	7.03s	7.10s	7.01s	7.00s	7.01s	7.04s	-	-
8	–	–	–	–	–	–	–	–	–	7.33s	–
1a	4.37d(7.0)	4.63d(9.5)	4.58d(7.5)	4.58d(7.0)	4.23 m	4.79d(6.5)	4.79d(6.5)	4.21 m	4.30 m	–	3.77d(7.0)
		4.36t(9.0)	3.92t(8.5)	3.92t(8.5)	3.84 m				3.98t(7.5,2.5)		
2a	5.58t(7.0)	3.66d(7.0)	3.62d(6.5)	3.62 m	3.73 m	5.77t(1.5)	5.76t(5.0,1.5)	1.86 m,1.55 m	4.33 m	–	5.13d
3a	–	–	–	–	–	–	–	2.59 m	–	–	–
4a	1.74s	1.07s	1.05(3H,s)	1.05(3H,s)	1.13(3H,s)	1.56(3H,s)	1.55(3H,s)	0.89(3H,s)	1.72 (3H,s)	–	1.81(3H,s)
5a	1.74s	1.14s	1.15(3H,s)	1.15(3H,s)	1.40(3H,s)	3.80s	3.80s	3.30 m	5.50s; 4.88s	–	1.64 (3H,s)
2′	7.64d(2.0)	8.10s	7.78d(1.5)	7.78d(2.0)	7.84d(2.0)	7.77d(2.0)	7.78d(2.0)	7.76s	7.77d(2.0)	8.02d(2.5)	8.07 d(2.0)
3′	6.77d(2.0)	7.63s	6.77d(2.0)	6.78d(2.0)	6.77d(2.0)	6.76d(2.0)	6.76d(2.5)	6.76s	6.77d(2.0)	7.39d(2.0)	7.14 d(2.5)
–OC<u>H</u>$_3$	–	–	–	3.57(3H,s)	–	–	3.57(3H,s)	–	–	4.26(3H,s)	–
Glc1″	–	–	–	–	–	–	–	–	–	–	5.54d(7.5)
Glc2″	–	–	–	–	–	–	–	–	–	–	3.35 m
Glc3″	–	–	–	–	–	–	–	–	–	–	3.20 m
Glc4″	–	–	–	–	–	–	–	–	–	–	3.20 m
Glc5″	–	–	–	–	–	–	–	–	–	–	3.30 m
Glc6″	–	–	–	–	–	–	–	–	–	–	3.52 m
											3.38 m

Table 2
^{13}C NMR spectral data for **IMP** and **1–10** (DMSO-d_6, 150 MHz, δ in ppm, J in Hz).

C	Imperatorin	1	2	3	4	5	6	7	8	9	10
2	160.2	159.8	174.0	172.8	173.8	174.1	172.9	174.0	174.1	160.0	159.5
3	114.2	114.1	33.9	33.6	34.2	34.0	33.6	33.9	34.1	112.2	113.8
4	144.3	145.2	25.8	25.8	26.1	26.0	25.9	26.0	25.9	139.4	141.9
5	113.2	113.6	114.6	114.7	114.2	114.5	114.5	114.4	114.8	149.4	113.6
6	125.7	125.8	120.2	120.3	123.5	120.2	120.3	120.3	120.3	112.4	125.4
7	148.3	147.7	145.3	145.3	144.7	145.6	145.6	145.4	145.2	157.7	145.9
8	131.2	131.6	131.4	131.4	136.9	131.2	131.2	131.4	131.2	93.1	127.1
9	143.5	142.5	144.1	144.1	142.8	144.4	144.4	144.1	144.1	152.1	142.8
10	116.2	116.4	124.5	124.1	130.3	125.0	124.6	125.0	124.8	105.6	125.9
1a	69.8	75.4	75.1	75.1	71.4	68.6	68.6	71.1	76.3	–	27.3
2a	119.7	76.7	75.9	75.8	74.1	118.9	118.8	32.9	72.7	–	125.5
3a	139.2	70.8	70.6	70.5	80.8	140.3	140.3	33.2	144.3	–	131.9
4a	17.8	24.5	24.2	24.2	19.8	13.5	13.5	16.9	18.6	–	17.9
5a	25.5	27.2	27.6	27.6	26.7	65.5	65.5	66.1	111.8	–	25.3
2′	146.4	147.1	144.3	144.3	145.6	144.2	144.3	144.2	144.3	145.8	147.2
3′	106.6	107.0	106.7	106.7	106.7	106.6	106.6	106.6	106.7	105.6	105.9
–O<u>C</u>H$_3$			–	51.2		–	51.1	–	–	60.2	–
Glc1″											101.9
Glc2″											73.8
Glc3″											77.5
Glc4″											69.6
Glc5″											76.7
Glc6″											60.5

2.9. In vitro anti-osteoporosis activity

Mouse osteoblastic cell line (MC3T3-E1, purchased from the Chinese Academy of Sciences Cell Bank) was cultured under a humidified atmosphere of 5% CO_2 at 37 °C with Dulbecco's modified Eagle's medium (DMEM) containing 1% penicillin streptomycin (Gibco) and 10% foetal bovine serum. The medium was refreshed every 2 days. After reaching confluence, the cells were subcultured using 0.02% EDTA–0.05% trypsin solution. Cell proliferation was determined by an assay using 3-(4,5-dimethylthiazol-2-yl)-2,5-diphenyltetrazolium bromide (MTT). The cells pre-cultured in growth media for 24 h at 5% CO_2, 37 °C, were treated with different concentrations (1, 10 and 100 μM) of the target compounds for 24 h. Then, MTT (5 mg/mL) was added to the cell cultures, and the samples were incubated for 4 h at 37 °C. In addition, the cells in normal culture medium were treated with the same volume of DMSO, similar to the test concentration of purified metabolites (**1–10**) as blank. Finally, the absorbance was measured in an optical 96-well microplate reader at a wavelength of 570 nm (Tai et al., 2010). Icariside was used as the positive control.

3. Results and discussion

In the present study, **IMP** was added to the 36-h precultures of *P. janthinellum* AS 3.510 followed by a further incubation of 5 days. A blank culture control and substrate control were used as described above. A total amount of 800 mg of substrate was used for the preparative-scale biotransformation. Ten products were isolated by the preparative chromatographic methods. Based on the ^{1}H NMR, ^{13}C NMR and 2D-NMR spectra, their chemical structures were elucidated as 2*a*,3*a*-dihydroxyimperatorin (**1**), 6,7-furano-8-(2*a*,3*a*-dihydroxyprenyloxy)hydrocoumaric acid (**2**), 6,7-furano-8-(2*a*,3*a*-dihydroxyprenyloxy)hydrocoumaric acid methyl ester (**3**), 6,7-furano-8-(2*a*-hydroxy-3*a*,9-epoxyprenyloxy)hydrocoumaric acid (**4**), 6,7-furano-8-(4*a*-hydroxymethylprenyloxy)hydrocoumaric acid (**5**), 6,7-furano-8- (4*a*-hydroxymethylprenyloxy)hydrocoumaric acid methyl ester (**6**), 6,7-furano-8- (4*a*-hydroxymethyl-2a,3a-dihydroprenyloxy)hydrocoumaric acid (**7**), 6,7-furano-8- (2*a*-hydroxy-3*a*-en-prenyloxy)hydrocoumaric acid (**8**), bergapten (**9**), and 6,7-furano- 5-isopentylcoumarin 8-*O*-*β*-D-glucoside (**10**). Among them, eight metabolites (**2**–**8** and **10**) were novel (Fig. 1).

Compounds **1** and **9** were identified as 2*a*,3*a*-dihydroxyimperatorin and bergapten, respectively. Their ^{1}H NMR and ^{13}C NMR spectral data were in agreement with those reported in the literature (Harkar, Razdan, & Waight, 1984; Liu, Feng, Sun, & Kong, 2004).

Compound **2** was obtained as yellow powder (MeOH). Its molecular formula of $C_{16}H_{20}O_7$ was established from high-resolution electrospray ionisation mass spectrometry (HRESIMS); a quasi-molecular ion $[M–H]^-$ was observed at *m/z* 323.1135. Compared with **IMP**, ^{13}C NMR spectrum of **2** exhibited the disappearance of olefinic carbons at δ 144.3 (C-4), δ 114.2 (C-3), δ 119.7 (C-2a), and δ 139.2 (C-3a), while the additional oxygenated methylenes at δ 75.9 and δ 75.1, and the aliphatic carbon signals of δ 25.8 and δ 33.9 were observed. It was also found that C-2 (δ 174.0) and C-10 (δ 124.6) shifted downfield Δ +13.8 ppm and Δ +8.3 ppm. All these evidences implied hydroxylation of the double bond, and hydrolysis of the lactone ring. In HMBC spectrum, CH_3-4a (δ 1.05) had long-range correlations with C-5a (δ 27.6), C-3a (δ 70.6) and C-2a (δ 75.9), and H-1a (δ 3.92) had HMBC correlations with C-2a (δ 75.9) and C-8 (δ 131.4). This indicated that two hydroxyl groups were located at C-2a and C-3a, respectively. In addition, the HMBC cross-peaks of H-3 (δ 2.51) with C-10 (δ 124.5) and C-4 (δ 25.8) were observed, and H-4 (δ 2.84) had HMBC correlations with C-3 (δ 33.9), C-5 (δ 114.6), C-9 (δ 144.1) and C-10 (δ 124.5), indicating the reduction of C-3,4 double bond and the hydrolysis of a lactone ring. The proton signal of δ 8.78 (OH) had HMBC correlations with C-10 (δ 124.5), C-8 (δ 131.4) and C-9 (δ 144.1), suggesting a hydroxyl group was located at C-9. Based on the above analysis, compound **2** was identified as 6,7-furano-8-(2*a*,3*a*-dihydroxyprenyloxy)hydrocoumaric acid. All the ^{1}H and ^{13}C NMR spectral data were unequivocally assigned by 2D NMR spectra (see Tables 1 and 2).

Compound **3** was isolated as a yellow powder (MeOH). Its molecular formula was determined as $C_{17}H_{22}O_7$ by HRMS. Compared to metabolite **2**, only an additional carbon signal of methoxyl group at δ 51.2 was observed in ^{13}C NMR spectrum of **3**. In the HMBC experiment, this methoxyl signal of δ 3.57 showed long-range correlations with C-2 (δ 172.8), suggesting that a methoxyl group was substituted at C-2. Therefore, compound **3** was identified as 6,7-furano-8(2*a*,3*a*-dihydroxyprenyloxy)hydrocoumaric acid methyl ester. All the ^{1}H and ^{13}C NMR spectral data were unambiguously assigned by 2D NMR spectra (see Tables 1 and 2).

Compound **4** was isolated as yellow powder (MeOH). HRMS suggested a molecular formula of $C_{16}H_{18}O_6$. Compared to **2**, the characteristic proton signal of δ 8.78 disappeared in ^{1}H NMR spectrum of **4**. Meantime, the ^{13}C NMR spectrum of **4** exhibited the oxygen-bearing carbon signals of δ 80.8 and δ 74.1. In the HMBC spectrum, correlations of the proton signal of δ 5.57 with C-1a (δ 71.4), C-2a (δ 74.1) and C-3a (δ 80.8) were observed. These data indicated the dehydration of two hydroxyl groups at C-9 and C-3a to form a new six-membered ring. On the basis of the above analysis, compound **4** was identified as 6,7-furano-8-(2*a*-hydroxy-3*a*,9-epoxyprenyloxy)hydrocoumaric acid.

Compound **5** was obtained as yellow powder (MeOH). HRMS suggested a molecular formula of $C_{16}H_{18}O_6$. When compared with **2**, additional carbon signals of δ 118.9 and δ 140.3, and only one oxygen-bearing carbon of δ 65.5 were observed. A methyl carbon signal at δ 25.5 disappeared in the ^{13}C NMR spectrum of **5**. In HMBC spectrum, H-4a (δ 3.80) was correlated with C-2a (δ 118.9), C-3a (δ 140.3) and C-5a (δ 13.5), while H-1a (δ 4.79) showed HMBC correlations with C-8 (δ 131.2), C-3a (δ 140.3) and C-2a (δ 118.9). These findings suggested that a hydroxyl group was substituted at C-4a. Thus compound **5** was identified as 6,7-furano-8-(5*a*-hydroxyl-methyl-prenyloxy)hydrocoumaric acid.

Compound **6** was isolated as yellow powder (MeOH). HRMS suggested a molecular formula of $C_{17}H_{20}O_6$. The spectral data of **6** were found to be very similar to those of **5**, except for an additional methoxyl group at δ 51.1. In the HMBC spectrum, the proton signal of δ 3.57 was found to be correlated with C-2 (δ 172.9), suggesting that a methoxyl group was located at C-2. Hence, compound **6** was identified as 6,7-furano-8-(5a-hydroxymethyl-prenyloxy) hydrocoumaric acid methyl ester.

Compound **7** was obtained as yellow powder (MeOH). HRMS data suggested a molecular formula of $C_{16}H_{20}O_6$. When compared with **5**, the ^{13}C NMR spectrum of **7** showed the absence of olefinic carbon signals of δ 118.9 and δ 140.3, suggesting the reduction of the side chain double bond. In the HMBC spectrum, H-5a had long-range correlations with C-3a (δ 33.2) and C-4a (δ 66.1). These evidences implied that the double bond of C-2a and C-3a was reduced. Consequently, compound **7** was identified as 6,7-furano-8-(4a-hydroxymethyl-3a,4a-dihydroprenyloxy) hydrocoumaric acid.

Compound **8** was obtained as yellow powder (MeOH). HRMS suggested a molecular formula of $C_{16}H_{18}O_6$. Similarly to **IMP**, the oxo group of C-2 (δ 160.2) shifted downfield to δ 174.1 in the ^{13}C NMR spectrum. An additional carbon signal of δ 72.7 was observed. In the HMBC spectrum, H-4 (δ 2.83) had long-range correlations with C-3 (δ 34.1), C-5 (δ 114.8), C-9 (δ 144.1), C-10 (δ 124.8), and C-2 (δ 174.1). These observations suggested that the lactone ring was hydrolysed. In addition, H-4a (δ 1.72) showed HMBC correlations with C-2a (δ 72.7), C-3a (δ 111.8) and C-5a (δ 144.3), indicating rearrangement of the double bond at C-3a and C-5a. In addition, H-5a (δ 5.50 and δ 4.88) had HMBC correlations with C-4a (δ 18.6) and C-2a (δ 72.7), while H-1a (δ 3.98) was correlated with C-2a (δ 72.7) and C-8 (δ 131.2). All this evidence suggested that the hydroxyl group was located at C-2a. Therefore, compound **8** was identified as 6,7-furano-8-(2a-hydroxy-3a-en-prenyloxy) hydrocoumaric acid.

Compound **10** was isolated as yellow powder (MeOH), with a suggested molecular formula of $C_{22}H_{25}O_9$. In the ^{13}C NMR spectrum the additional carbon signals of δ 60.5, δ 69.6, δ 73.8, δ 76.7, δ 77.5 and δ 101.9 indicated that a sugar moiety was introduced in the chemical structure of **10**. The sugar moiety was identified as D-glucose by chemical hydrolysis. The anomeric proton coupling constant of 7.5 Hz and anomeric carbon signal of δ 101.9 (C-1) suggested that the configuration of glucopyranosyl should be β. In the HMBC spectrum, the proton signal of δ 5.54 was observed to be correlated with C-8 (δ 127.1), indicating that the glucopyranosyl moiety should be at C-8. In the HMBC spectrum, H-4a (δ 1.81) was found to be correlated with C-5a (δ 25.3), C-2a (δ 125.5) and C-3a (δ 131.9), while H-1a (δ 3.77) had HMBC correlations with C-5 (δ 113.6), C-6 (δ 125.4), C-2a (δ 125.5), C-3a (δ 131.9) and C-10 (δ 125.9). The findings suggested that an isopentane group was located at C-5. On the basis of above analysis, the chemical structure of compound **10** was identified as 6,7-furano-5-isopentyl-coumarin 8-*O*-β-D-glucoside. All the ^{1}H and ^{13}C NMR spectral data were assigned by 2D NMR spectra (see Tables 1 and 2).

A previous report showed that *Glomerello cingulata* could metabolise some coumarins such as isopimpinellin, bergapten, xanthotoxin and isoimperatorin, to the corresponding reduced acid (Marumoto and Miyazawa, 2010b, 2010c, 2011a, 2011b), while **IMP**, as a specific coumarin with a prenyloxy side-chain, could be transformed by *G. cingulata* to yield the dealkylated metabolite xanthotoxol in high yield (81%), rather than the corresponding reduced acid derivatives. In addition, **IMP** could also be metabolised by *Aspergillus flavus* to form products specifically oxidised at C-4a and C-5a positions with xanthotoxol as a minor metabolite, producing cleavage at the prenyloxy side-chain (Teng, Huang, Huang, Chung, & Chen, 2004).

In our present work, *P. janthinellum* exhibited a great capability to transform **IMP** into a series of novel transformed products, most of which were the corresponding derivatives of hydrocoumaric

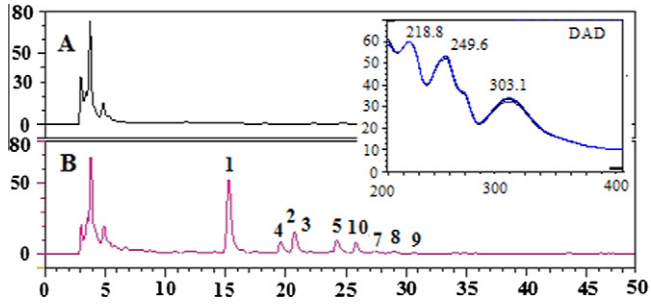

Fig. 2. HPLC chromatograms of the blank of *P. janthinellum* AS 3.510 (A) and administrating **IMP** for 5 days (B). All UV spectra were similar to that of metabolite **1**.

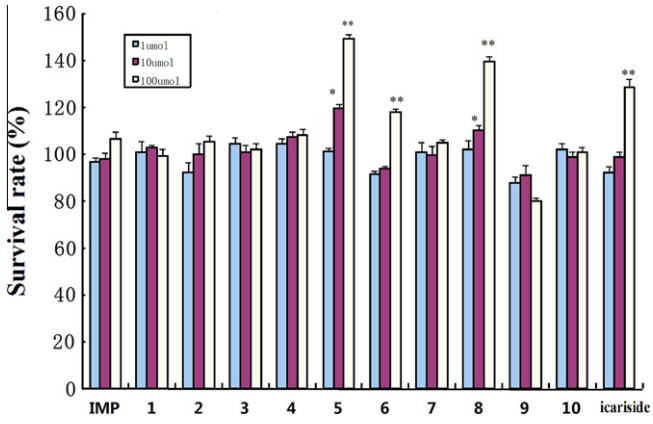

Fig. 3. The transformed products and **IMP** effects on osteoblast proliferation in MC3T3-E1 cells by MTT method.

acid (Fig. 2). The major bioreactions involved the hydroxylation of the isopentenyl group, and hydrolysis and reduction at the α,β-unsaturated lactone ring of a furocoumarin skeleton. In addition, dehydration, glycosylation, methylation and rearrangement of double bond were also observed as minor reactions of **IMP**. The biotransformation pathway of **IMP** metabolised by *P. janthinellum* AS 3.510 is illustrated in Fig. 1.

In addition, the effects of transformed products (**1**–**10**) and **IMP** on osteoblast function by using MC3T3-E1 cell line at concentrations of 1, 10 and 100 μM were investigated (Fig. 3). At concentrations of 1 and 10 μM, almost no transformed products could increase MC3T3-E1 cell growth. Interestingly, at 100 μM, products **5**, **6** and **8** could increase MC3T3-E1 cell growth, with survival rates of 175.5%, 118.35% and 145.3%, respectively. Our results indicated that the skeleton of hydrocoumaric acid with an isopentene group hydroxylated at C-5a, such as products **5** and **6** had better bioactivity in MC3T3-E1 cell growth than **IMP**. Also, the double bond of prenyloxy side-chain was found to be very important for the biological activity. Derivatives of hydrocoumaric acid after hydroxylation of the double bond of C-2a and C-3a (such as in compounds **2** and **3**) did not enhance MC3T3-E1 cell growth. Compound **9**, as a dealkylated metabolite, showed significant inhibition of MC3T3-E1 cell growth at all concentrations, suggesting the isopentene moiety was vital for the anti-osteoporosis activities.

4. Conclusions

The incubation of **IMP** with *P. janthinellum* AS 3.510 yielded ten products in total, including eight previously unreported metabolites. The enzymatic reactions included hydrolysis and reduction at α,β-unsaturated lactone ring, hydroxylation, methylation, dehydration and glycosylation, which were observed for the first time in microbial transformation processes of **IMP**. Some novel metabolites (**5** and **8**) showed potent bioactivity in increasing MC3T3-E1 cell growth. Hence, these metabolites could be used as potent candidates for the further development of anti-osteoporosis drugs or functional foods.

Acknowledgements

We thank the National Natural Science Foundation of China (No. 81274047), Personnel Department of Liaoning province and the Program for Liaoning Excellent Talents (LJQ2011095) in the University, the Education Department of Liaoning Province (LS2010059) for funding towards this research.

Appendix A. Supplementary data

Supplementary data associated with this article can be found, in the online version, at http://dx.doi.org/10.1016/j.foodchem.2012.11.138.

References

Deng, S., Zhang, B. J., Wang, C. Y., Tian, Y., Yao, J. H., An, L., et al. (2012). Microbial transformation of deoxyandrographolide and their inhibitory activity on LPS-induced NO production in RAW 264.7 macrophages. *Bioorganic & Medicinal Chemistry Letters, 22*, 1615–1618.

Garcia-Argaez, A. N., Ramirez-Apan, T. O., Delgado, H. P., Velazquez, G., & Martinez-Vazquez, M. (2000). Anti-inflammatory activity of coumarins from *Decatropis bicolor* on TPA ear mice model. *Planta Medica, 66*, 279–281.

Harkar, S., Razdan, T. K., & Waight, E. S. (1984). Steroids, chromone and coumarins from *Angelica officinalis*. *Phytochemistry, 23*, 419–426.

He, J. Y., Zhang, W., He, L. C., & Cao, Y. X. (2007). Imperatorin induces vasodilatation possibly via inhibiting voltage dependent calcium channel and receptor-mediated Ca^{2+} influx and release. *European Journal of Pharmacology, 573*, 170–175.

Kim, Y. K., Kim, Y. S., & Ryu, S. Y. (2007). Antiproliferative effect of furanocoumarins from the root of *Angelica dahurica* on cultured human tumor cell lines. *Phytotherapy Research, 21*, 288–290.

Li, Y. B. (2006). Determination of imperatorin in rat plasma by reversed-phase high performance liquid chromatography after oral administration of *Radix Angelicae dahuricae* extract. *Journal of Pharmaceutical and Biomedical Analysis, 40*, 1253–1256.

Li, F. Y., Cang, P. R., Huang, S. S., Zhang, B. J., Xin, X. L., Yao, J. H., et al. (2011). Microbial transformation of deoxyandrographolide by *Cunninghamella echinulata*. *Journal of Molecular Catalysis B: Enzymatic, 68*, 187–191.

Liu, R. M., Feng, L., Sun, A. L., & Kong, L. Y. (2004). Preparative isolation and purification of coumarins from *Cnidium monnieri* (L.) Cusson by high-speed counter-current chromatography. *Journal of Chromatography, A, 1055*, 71–76.

Ma, X. C., Cui, J., Zheng, J., & Guo, D. A. (2007). Microbial transformation of three bufadienolides by *Penicillium aurantigriseum* and its application for metabolite identification in rat. *Journal of Molecular Catalysis B: Enzymatic, 48*, 42–50.

Ma, X. C., Ning, J., Ge, G. B., Liang, S. C., Wang, X. L., Zhang, B. J., et al. (2011). Comparative metabolism of cinobufagin in liver microsomes from mouse, rat, dog, minipig, monkey, and human. *Drug Metabolism and Disposition, 39*, 675–682.

Ma, X. C., Wu, L. J., & Guo, D. A. (2006). Microbial transformation of curdione by *Mucor spinosus*. *Enzyme and Microbial Technology, 38*, 367–371.

Ma, X. C., Xin, X. L., Liu, K. X., Han, J., & Guo, D. A. (2008). Microbial transformation of cinobufagin by *Syncephalastrum racemosum*. *Journal of Natural Products, 71*, 1268–1270.

Ma, X. C., Zheng, J., & Guo, D. A. (2007). Highly selective isomerization and dehydrogenation of three major bufadienolides at 3-OH by *Fusarium solani*. *Enzyme and Microbial Technology, 40*, 1585–1591.

Marumoto, S., & Miyazawa, M. (2010a). The β-secretase inhibitory effects of furanocoumarins from the root of *Angelica dahurica*. *Phytotherapy Research, 24*, 510–513.

Marumoto, S., & Miyazawa, M. (2010b). Biotransformation of Bergapten and Xanthotoxin by *Glomerella cingulata*. *Journal of Agricultural and Food Chemistry, 58*, 7777–7781.

Marumoto, S., & Miyazawa, M. (2010c). Biotransformation of isoimperatorin and imperatorin by *Glomerella cingulata* and β-secretase inhibitory activity. *Bioorganic & Medicinal Chemistry, 18*, 455–459.

Marumoto, S., & Miyazawa, M. (2011a). Microbial transformation of isoimpinellin by *Glomerella cingulata*. *Journal of Oleo Science, 60*, 575–578.

Marumoto, S., & Miyazawa, M. (2011b). Microbial reduction of coumarin, psoralen, and xanthyletin by *Glomerella cingulata*. *Tetrahedron, 67*, 495–500.

Rosselli, S., Maggio, A., Bellone, G., Formisano, F., Basile, A., Cicala, C., et al. (2006). Antibacterial and anticoagulant activities of coumarins isolated from flowers of *Magydaris tomentosa*. *Planta Medica, 72*, 116–120.

Shin, K. H., & Woo, W. S. (1986). Inhibition of hepatic microsomal drug-metabolizing enzymes by imperatorin. *Archives of Pharmacal Research, 9*, 81–86.

Tai, B. H., Huyen, V. T., Huong, T. T., Nhiem, N. X., Choi, E. M., Kim, J. A., et al. (2010). New pyrano-pyrone from *Goniothalamus tamirensis* enhances the proliferation and differentiation of osteoblastic MC3T3-E1 cells. *Chemical & Pharmaceutical Bulletin, 58*, 521–525.

Tang, C. H., Yang, R. S., Chen, M. Y., Chen, C. C., & Fu, W. M. (2008). Enhancement of bone morphogenetic protein-2 expression and bone formation by coumarin derivatives via p38 and ERK-dependent pathway in osteoblasts. *European Journal of Pharmacology, 579*, 40–49.

Teng, W. Y., Huang, Y. L., Huang, R. L., Chung, R. S., & Chen, C. C. (2004). Biotransformation of imperatorin by *Aspergillus flavus*. *Journal of Natural Products, 67*, 1014–1017.

Zhang, Y., Cao, Y. J., Zhan, Y. Z., Duan, H. J., & He, L. C. (2010). Furanocoumarins-imperatorin inhibits myocardial hypertrophy both *in vitro* and *in vivo*. *Fitoterapia, 81*, 1188–1195.

Zhang, Q. Y., & Qin, L. P. (2003). Study on effects of total coumarines from the fruits of *Cnidium monnieri* on osteoporosis in ovariectomized rats. *Chinese Pharmaceutics, 38*, 101–103.